

# Sonogenetic-Based Neuromodulation for the Amelioration of Parkinson's Disease

Ching-Hsiang Fan,<sup>▲</sup> Kuo-Chen Wei,<sup>▲</sup> Nai-Hua Chiu, En-Chi Liao, Hsien-Chu Wang, Ruo-Yu Wu, Yi-Ju Ho, Hong-Lin Chan, Tsung-Shing Andrew Wang, Ying-Zu Huang, Tsung-Hsun Hsieh, Chin-Hsien Lin, Yu-Chun Lin,\* and Chih-Kuang Yeh\*



Cite This: <https://doi.org/10.1021/acs.nanolett.1c00886>



Read Online

ACCESS |



Metrics & More



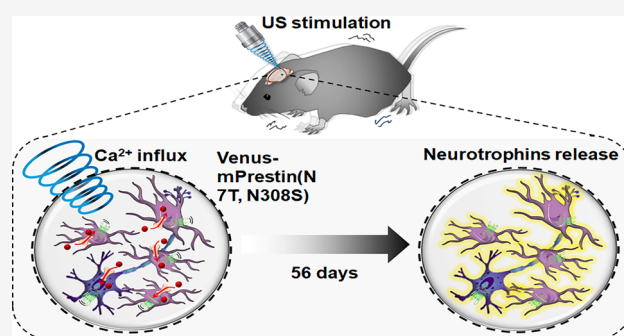
Article Recommendations



Supporting Information

**ABSTRACT:** Sonogenetics is a promising strategy allowing the noninvasive and selective activation of targeted neurons in deep brain regions; nevertheless, its therapeutic outcome for neurodegeneration diseases that need long-term treatment remains to be verified. We previously enhanced the ultrasound (US) sensitivity of targeted cells by genetic modification with an engineered auditory-sensing protein, mPrestin (N7T, N308S). In this study, we expressed mPrestin in the dopaminergic neurons of the substantia nigra in Parkinson's disease (PD) mice and used 0.5 MHz US for repeated and localized brain stimulation. The mPrestin expression in dopaminergic neurons persisted for at least 56 days after a single shot of adeno-associated virus, suggesting that the period of expression was long enough for US treatment in mice. Compared to untreated mice, US stimulation ameliorated the dopaminergic neurodegeneration 10-fold and mitigated the PD symptoms of the mice 4-fold, suggesting that this sonogenetic strategy has the clinical potential to treat neurodegenerative diseases.

**KEYWORDS:** sonogenetics, ultrasound, Parkinson's disease, dopaminergic neuron, ultrasound-sensing protein



The selective stimulation of targeted neurons could be beneficial to our understanding of central nervous system (CNS) function and provides therapeutic opportunities for brain pathologies. For instance, Parkinson's disease (PD), one of the most common neurodegenerative disorders, involves a continuous loss of dopaminergic neurons in the substantia nigra (SN).<sup>1,2</sup> Current PD treatments are limited to the long-term use of dopaminergic medications, which do not limit disease progression.<sup>3,4</sup> Selective stimulation of dopaminergic neurons provides an alternative approach to improving downstream motor circuit control, ameliorating motor dysfunction through increased dopamine release, and activating neuronal plasticity mechanisms.<sup>5–9</sup> Currently, brain neuron stimulation relies on invasively implanted electrodes, which pose concerns of infection or invasive damage.<sup>10,11</sup> The alternatives that rely on electromagnetic induction, chemogenetics, or optogenetics have been hindered by low spatial resolution, systemic drug administration, and high tissue absorption.<sup>12,13</sup> Here, we have developed a unique spatially targeted and cell-specific neuromodulation technology using transcranial focused ultrasound (US) and an engineered US-sensing protein, mPrestin (N7T, N308S), from an echolocating species.

US has been shown to have neuromodulatory properties and beneficial effects to accelerate axonal neurogenesis in the

damaged neurons or hippocampus.<sup>14,15</sup> US could also increase the production of endogenous neurotrophins, growth factors, and brain-derived neurotrophic factor (BDNF) for the amelioration of Alzheimer's disease and traumatic brain injury in mice.<sup>16,17</sup> In order to initiate regeneration, some studies are performed either with long-term sonication (600–900 s) or in combination with microbubbles because of the natural US-insensitive property of neurons. Furthermore, the submillimeter spatial resolution of US might affect the activity of untargeted neurons and trigger immune responses.

To circumvent the limitations of current approaches to US-induced neuroregeneration, we recently proposed a sonogenetic strategy to enhance the US-responsive capability of certain neurons.<sup>18</sup> This method relies on genetic modifications of the naturally occurring US-sensing prestin proteins, which are expressed in the outer hair cells of cochlea in echolocating mammals and are responsible for high-frequency hearing.<sup>19,20</sup>

**Received:** March 4, 2021

**Revised:** July 7, 2021

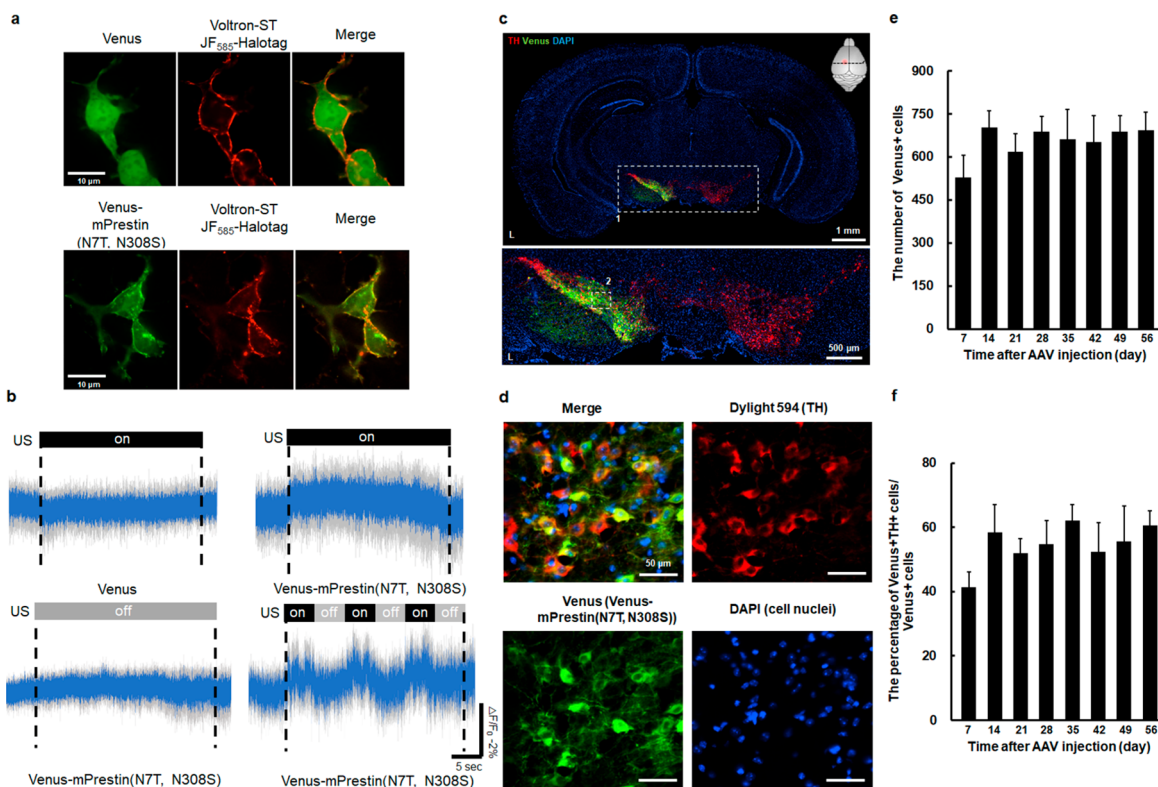


**Figure 1.** US stimulation changed the membrane potential of cells expressing Venus-mPrestin (N7T, N308S) and the in vivo expression of Venus-mPrestin (N7T, N308S) in dopaminergic neurons. (a) Representative live-cell images of SH-SY5Y cells coexpressing Voltron-ST with Venus-mPrestin (N7T, N308S) or Venus as a control. Transfected cells were treated with 100 nM JF585-HaloTag for 1 h to visualize Voltron-ST. (b) Relative fluorescence intensity change in Venus-expressing or Venus-mPrestin (N7T, N308S)-expressing cells with and without US stimulation. Single stimulation of Venus-mPrestin (N7T, N308S) transfected cells showed a single fluorescence change with US stimulation (upper panel). Multiple US stimulation also could repeatedly change the membrane potential in Venus-mPrestin (N7T, N308S)-expressing cells (bottom panel). Neither the Venus+US group nor Venus-mPrestin (N7T, N308S) alone observed a fluorescence change during the recording. Data are presented as the mean  $\pm$  SEM (gray),  $n = 7$  and 6 cells from three independent experiments in the Venus group and the Venus-mPrestin (N7T, N308S) group, respectively. (c) Representative immunohistology of SN with TH (red), Venus-mPrestin (N7T, N308S) (yellow), and nucleus (DAPI, blue) staining at 7 days after AAV injection in healthy mice. Top: whole brain section. Bottom: magnification of ROI1. (d) Magnification of ROI2. Orange color: overlap of the Venus-mPrestin (N7T, N308S) signal and TH signal. (e) Representative number of Venus+ cells at each time point. (f) Percentage of Venus+TH+ cells/Venus+ cells at different time points after AAV injection. Data are presented as the mean  $\pm$  standard deviation ( $n = 3$  per time point).

The mutation of N7T and N308S enabled the mouse prestin protein (mPrestin (N7T, N308S))<sup>21</sup> to sensitize the US. Our previous results indicated that the expression of this construct improved the US sensitivity of targeted cells by  $\sim$ 11-fold compared to that of nonexpressing cells using low-frequency (0.5 MHz), transient (3 s), and low-energy (0.5 MPa) US parameters.

Although sonogenetics is a promising strategy allowing the noninvasive and selective activation of targeted neurons in deep brain areas, its therapeutic ability for neurodegenerative disease remains to be verified. Herein, we demonstrate this concept by using sonogenetics to selectively stimulate dopaminergic neurons in SN and verify the effects of repeated neuronal stimulation in wild-type healthy as well as genetic PD mice. We used motor function tests to evaluate the improvement in locomotor function and investigated the molecular mechanisms underlying sonogenetic stimulation in dopaminergic neurons.

## RESULTS

### 0.5 MHz US Stimulation Can Induce Membrane Potential Changes in Venus-mPrestin (N7T, N308S)-

**Expressing SH-SY5Y Cells.** We first tested whether 0.5 MHz US stimulation can activate neurons expressing Venus-mPrestin (N7T, N308S). For real-time monitoring of the membrane potential of cells receiving US stimulation, SH-SY5Y neuroblastoma cells were cotransfected with Venus-mPrestin (N7T, N308S) and Voltron-ST, a bright and photostable voltage biosensor that has been recently developed.<sup>22</sup> The Voltron-ST in cells was visualized using JF<sub>585</sub>-HaloTag dye (Figure S1), and its intensity was inversely correlated with the membrane potential of cells with submillisecond time resolution. Single excitation with US rapidly changed the membrane potential of cells expressing Venus-mPrestin (N7T, N308S) but not that of cells expressing only Venus (Figure 1a,b, upper panel). Multiple US stimulations repeatedly changed the membrane potential in Venus-mPrestin (N7T, N308S)-expressing cells (Figure 1b, bottom panel). Our previous study demonstrated that US stimulation triggers calcium influx in Venus-mPrestin (N7T, N308S)-expressing cells, which may in turn cause membrane depolarization.<sup>18</sup> This result confirmed that US stimulation can activate neuronal cells with Venus-mPrestin (N7T, N308S) expression by changing their membrane potential.

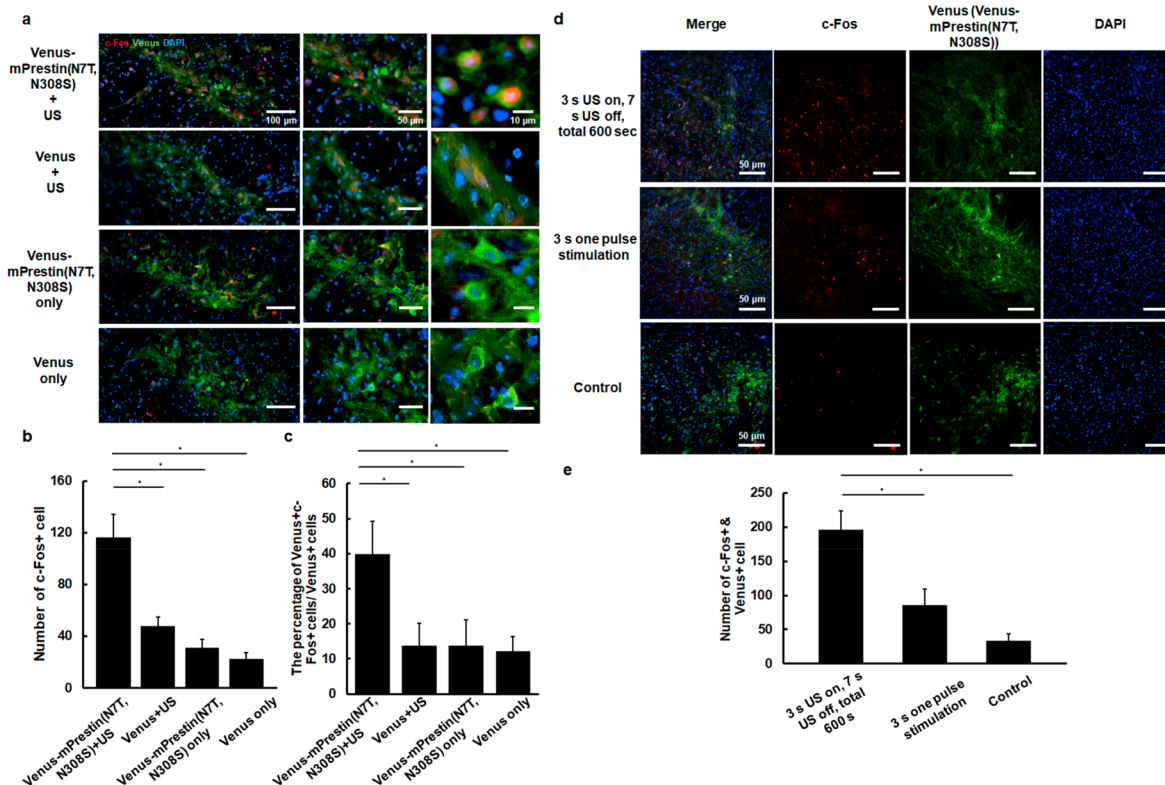


**Figure 2.** 0.5 MHz US stimulation can activate Venus-mPrestin (N7T, N308S)-transfected neurons. (a) Immunostaining for the activation of the Venus-mPrestin (N7T, N308S)-transfected area and non-Venus-mPrestin (N7T, N308S)-transfected area by US. (b) Representative number of c-Fos+ cells in each group. (c) Percentage of Venus+c-Fos+ cells/Venus+ cells in different stimulation groups. (d) c-Fos expression of the Venus-mPrestin (N7T, N308S)-transfected area with a different stimulation protocol. (e) Number of c-Fos+ and Venus+ cells in each group. Data are presented as the mean  $\pm$  standard deviation ( $n = 4$  per group) ( $*p < 0.05$ ).

**In Vivo Expression of Venus-mPrestin (N7T, N308S) in Dopaminergic Neurons.** Next, the intracerebral expression efficacy of Venus-mPrestin (N7T, N308S) in dopaminergic neurons of healthy mice was evaluated by microscopic imaging. Mouse brains were harvested and sliced at different time points after intracerebral gene transfection (days 7, 14, 21, 28, 35, 42, 49, and 56). The Venus yellow fluorescence signals started to appear in the expected location of the SN at 7 days after transfection (Figure 1c,d) and overlapped well with dopaminergic neurons (tyrosine hydroxylase [TH]; red fluorescence signal), as evidenced by the orange fluorescence signals. The number of Venus-expressing cells stabilized at 14 days following gene transfection (7 days,  $528 \pm 77.9$ ; 14 days,  $701.7 \pm 60.1$ ; 21 days,  $618.7 \pm 61.3$ ; 28 days,  $688 \pm 53.1$ ; 35 days,  $662 \pm 102.6$ ; 42 days,  $652.3 \pm 61.6$ ; 49 days,  $689 \pm 55.6$ ; and 56 days,  $694 \pm 61.5$ ) (Figure 1e). In contrast, no Venus-expressing cells were observed in the contralateral non-transfected site of SN. Following the confirmation of expression duration of Venus-mPrestin (N7T, N308S), we examined whether this gene transfection configuration resulted in the expression of Venus-mPrestin (N7T, N308S) in dopaminergic neurons, which were labeled with red fluorescence. Subsequent immunofluorescent imaging of SN sections revealed a high percentage of Venus+TH+ cells among Venus+ cells (7 days,  $41.3 \pm 4.7\%$ ; 14 days,  $58.3 \pm 8.7\%$ ; 21 days,  $52 \pm 4.6\%$ ; 28 days,  $54.7 \pm 7.4\%$ ; 35 days,  $62.0 \pm 5.0\%$ ; 42 days,  $52.3 \pm 9.1\%$ ; 49 days,  $55.7 \pm 10.9\%$ ; and 56 days,  $60.7 \pm 4.5\%$ ), suggesting the successful expression of mPrestin (N7T, N308S) in dopaminergic neurons (Figure 1f).

**0.5 MHz US Stimulation Can Activate Venus-mPrestin (N7T, N308S)-Transfected Neurons.** We then tested whether US could achieve reliable neuronal activation by staining for c-Fos-positive nuclei. The animals received US stimulation 9 days after intracerebral gene transfection. Compared with Venus-only expressing cells, c-Fos signals were enhanced in the mPrestin (N7T, N308S)-expressing cells after US stimulation, indicating the activation of neurons (Figure 2a,b) [Venus-mPrestin (N7T, N308S)+US group ( $118 \pm 18$ ) vs Venus+US group ( $48 \pm 7$ )]. In addition, c-Fos signals were rarely detected in the no US stimulation groups [Venus-mPrestin (N7T, N308S)-only group ( $31 \pm 6.2$ ) vs Venus-only group ( $22.3 \pm 5.1$ )]. We further verified that these c-Fos positive signals were from Venus-mPrestin (N7T, N308S)-transfected cells. The high colocalization between yellow fluorescence signals and red fluorescence signals in the Venus-mPrestin (N7T, N308S)+US group ( $39.3 \pm 9.4\%$ ) compared with the Venus+US group ( $13.7 \pm 6.4\%$ ), Venus-mPrestin (N7T, N308S) alone group ( $13.7 \pm 7.4\%$ ), and Venus alone group ( $12.2 \pm 4.0\%$ ) (Figure 2c) indicated that the US could selectively activate Venus-mPrestin (N7T, N308S)-expressing cells. Subsequently, we investigated if c-Fos induction could be enhanced by extending the duration of US stimulation. Figure 2d,e demonstrated a significant increase in the number of c-Fos-expressing cells in the longer stimulation group ( $195.6 \pm 28.5$ ,  $85.5 \pm 23.7$ , and  $33.4 \pm 10.1$  for the 600 s stimulation group, 3 s one-pulse stimulation-only group, and no stimulation control group, respectively). We therefore used the US protocol of 3 s US on, 7 s US off, total 600 s, weekly

stimulation, total of 8 weeks for the following animal stimulation.

**Repeated Neuronal Stimulation Promotes Neurotrophin Expression in PD Mice.** Next, we explored the effects of repeated neuronal stimulation on the expression of neuroprotective neurotrophic factors in left SN. We examined the expression of the activity-dependent neurotrophin family, including brain-derived neurotrophic factor (BDNF) and nerve growth factor (NGF), 56 days after gene transfection (Figure S2). PD was associated with a dramatic decrease in BDNF expression compared with healthy mice (Figure 3a). Western blot analysis showed that BDNF protein levels were obviously higher in US-stimulated mice, especially in Venus-mPrestin (N7T, N308S)-expressing mice (relative expression levels

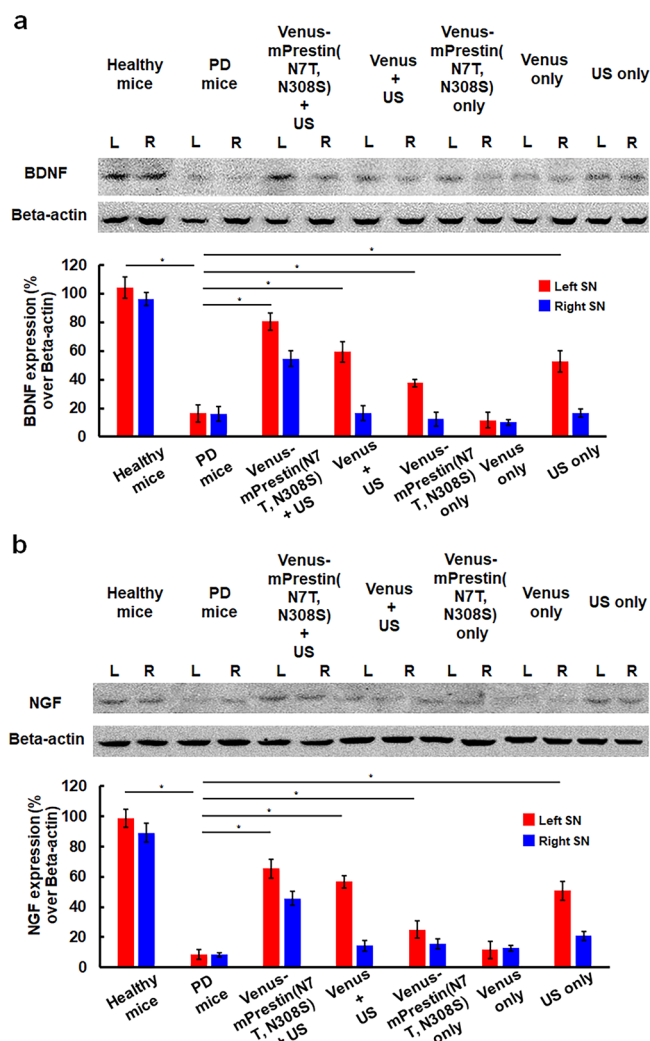


**Figure 3.** Neuronal stimulations increased BDNF and NGF expression in SN. The animals were sacrificed 56 days after starting treatment, and the left SNs within the brains were removed and analyzed. (a) Top: GDNF expression after different treatments as measured by Western blot analysis. Bottom: Quantification of GDNF expression in each group measured by ImageJ and expressed relative to  $\beta$ -actin expression ( $n = 5$  per group). (b) Top: NGF expression after different treatments measured by Western blot analysis. Bottom: Quantification of NGF expression in each group measured by ImageJ and expressed relative to  $\beta$ -actin expression ( $n = 5$  per group). All data were compared with those from PD mice. Data are presented as mean  $\pm$  standard deviation. (\*  $p < 0.05$ ).

normalized to  $\beta$ -actin: healthy mice,  $104.3 \pm 7.5\%$ ; PD mice,  $16.3 \pm 6.0\%$ ; US only in PD mice,  $52.7 \pm 7.2\%$ ; Venus only in PD mice,  $11.7 \pm 5.7\%$ ; Venus+US in PD mice,  $59.3 \pm 7.0\%$ ; Venus-mPrestin (N7T, N308S) in PD mice,  $37.6 \pm 2.5\%$ ; and Venus-mPrestin (N7T, N308S)+US in PD mice,  $80.7 \pm 6.0\%$ ). The expression of NGF (Figure 3b) was also significantly reduced in PD mice and significantly upregulated in US-stimulated Venus-mPrestin (N7T, N308S)-expressing mice compared to Venus-mPrestin (N7T, N308S)-expressing mice without US stimulation (relative expression levels normalized to  $\beta$ -actin: healthy mice,  $98.7 \pm 6.1\%$ ; PD mice,  $8.6 \pm 3.2\%$ ; US only in PD mice,  $50.1 \pm 6.1\%$ ; Venus only in PD mice,  $11.7 \pm 5.9\%$ ; Venus+US in PD mice,  $56.7 \pm 4.2\%$ ; Venus-mPrestin (N7T, N308S) only in PD mice,  $25.0 \pm 5.6\%$ ; and Venus-mPrestin (N7T, N308S)+US in PD mice,  $65.3 \pm 6.4\%$ ). The corresponding quantification data of the right SN are listed in Table S1. These data suggest that repeated neuronal stimulation would upregulate BDNF and NGF expression and potentially activate BDNF/NGF-facilitated synaptic plasticity.

**Repeated Neuronal Stimulations Mitigate Dopaminergic Neuronal Degeneration in PD Mice.** To histologically confirm the amelioration of dopaminergic neuronal degeneration after repeated neuronal stimulation in PD mice, we used IHC staining to examine the dopaminergic neuronal areas in the SN (Figure 4a). There was a significant loss of TH-positive neurons in bilateral SN in untreated PD mice ( $7.6 \pm 4.9\%$  compared with healthy mice). However, Venus-mPrestin (N7T, N308S)+US treatment remarkably slowed TH-positive neuron loss in SN ( $73.9 \pm 10.8\%$  compared with healthy mice, Figure 4a and statistics in Figure 4b), which was not observed in the Venus alone group ( $18.9 \pm 6.9\%$  compared with healthy mice) (Figure 4b). Treatment with US alone or with Venus+US provided some beneficial effects ( $39.4 \pm 7.8$  and  $36.1 \pm 1.9\%$ , respectively, compared with healthy mice). Notably, the Venus-mPrestin (N7T, N308S) alone group also showed some favorable effects ( $34.8 \pm 7.3\%$  compared with healthy mice). These data suggest that repeated US stimulation in Venus-mPrestin (N7T, N308S)-expressing neurons could mitigate neuronal loss in SN as a result of the enhanced neurotrophin expression.

The beneficial effect of dopaminergic neuronal loss by repeated US in Venus-mPrestin (N7T, N308S)-expressing nigral neurons was confirmed by TH expression and DOPA decarboxylase activity in SN. Previous studies have shown that the activity of DOPA decarboxylase is crucial to dopamine synthesis.<sup>23,24</sup> Western blot analysis confirmed that the PD mice had significantly reduced TH expression and DOPA decarboxylase expression ( $12.0 \pm 5.3$  and  $12.7 \pm 7.4\%$ ) compared with expression in the left SN of healthy mice ( $96.0 \pm 5.7$  and  $99.3 \pm 1.2\%$ , where the fold expression indicates expression relative to  $\beta$ -actin) (Figure 4c,d). However, treating PD mice with Venus-mPrestin (N7T, N308S)+US increased the expression of both TH and DOPA decarboxylase ( $81.3 \pm 4.2$  and  $68.0 \pm 7.2\%$ ) (Figure 4c,d). These findings suggest that the stimulated residual dopaminergic neurons in PD mice still have the potential to produce dopamine. It was noted that TH expression and DOPA decarboxylase expression were only slightly improved by treatment with Venus+US ( $55 \pm 10.4$  and  $55.3 \pm 4.5\%$ ) and US alone ( $45.0 \pm 4.6$  and  $35.3 \pm 4.9\%$ ), although this was superior to the Venus alone ( $14.7 \pm 6.4$  and  $10.0 \pm 4.0\%$ ) and Venus-mPrestin (N7T, N308S) ( $42.3 \pm 5.9$  and  $25.7 \pm 5.9\%$ ) groups. The corresponding quantification data for right SN are listed in Table S1. Taken together, these

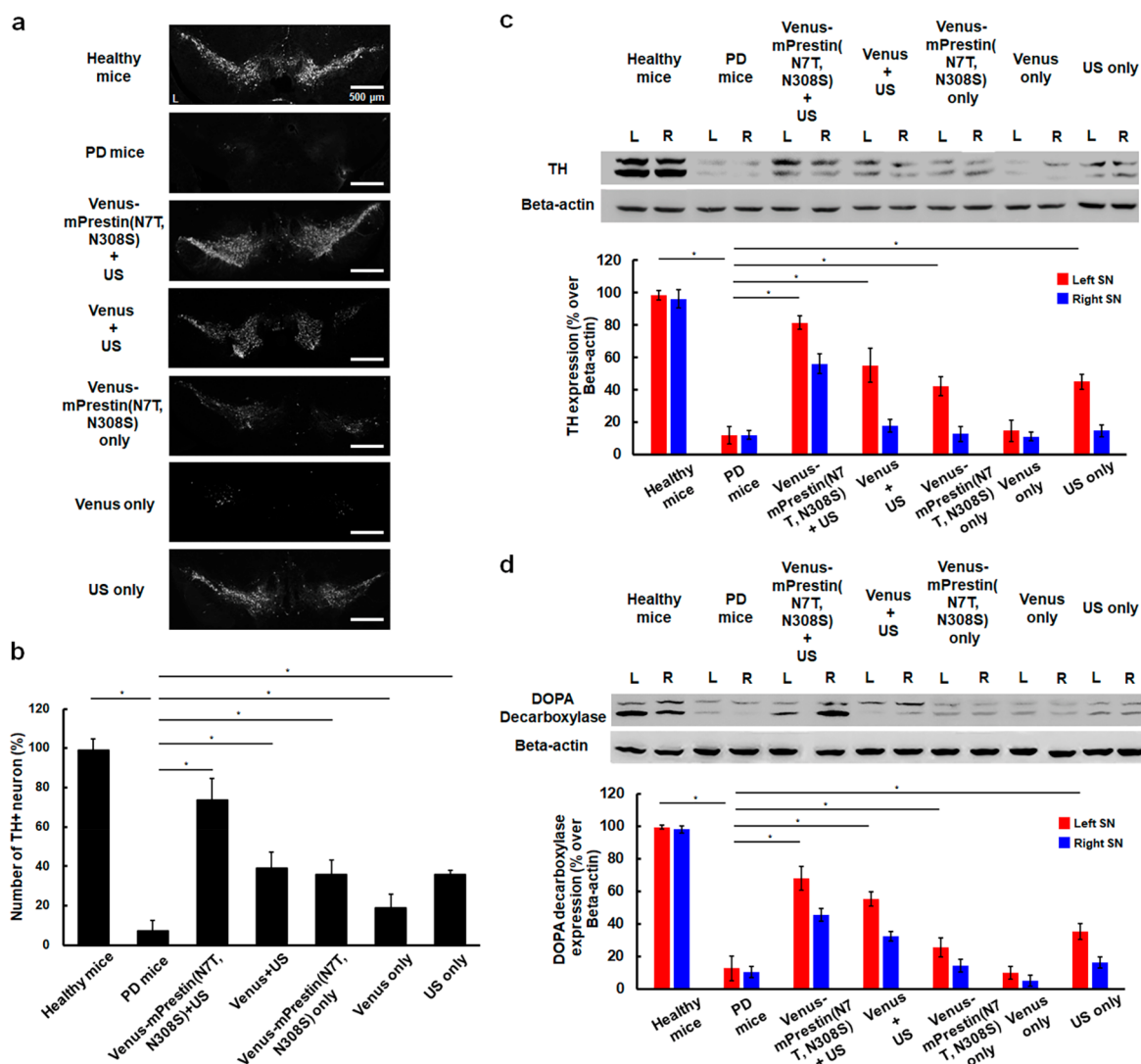


**Figure 4.** Repeated neuronal stimulations mitigate dopaminergic neuronal loss in PD mice. (a) Representative photomicrographs of SN sections immunostained for TH after treatment (post-PD day 56). (b) Number of TH+ cells in the treated animals compared to the healthy animals. All data were compared with those from untreated PD mice. (c) Top: Western blot of TH expression in the SN of nonstimulated and stimulated PD mice (post-PD day 56). Bottom: Relative optical density measurements of TH expression shown relative to  $\beta$ -actin expression. (d) Top: Western blot of DOPA decarboxylase expression in SN of nonstimulated and stimulated PD mice (post-PD day 56). Bottom: Relative optical density measurements of DOPA decarboxylase expression expressed relative to  $\beta$ -actin expression. Data are presented as the mean  $\pm$  standard deviation ( $n = 5$  per group) ( $*p < 0.05$ ).

data suggest that repeated neuronal stimulation may significantly upregulate BDNF and NGF expression and slow down the degeneration of dopaminergic neurons, in addition to improving the dopamine synthesis activity.

**Repeated Neuronal Stimulation Promotes Functional Behavioral Recovery in PD Mice.** MitoPark mice can exhibit several cardinal features of human PD, including age-dependent degeneration of nigrostriatal dopamine circuitry and a progressive decline in motor behaviors.<sup>25–27</sup> To address whether repeated neuronal stimulations of dopaminergic neurons can improve locomotor deficits in MitoPark mice, we examined the motor function of PD mice using the beam-walking and open field tests (Figure S2).

During the experimental period (days 0 to 35), motor performance in the beam-walking test largely decreased in untreated PD mice ( $10.2 \pm 2.8$  to  $32.9 \pm 10.2$  s;  $5816.5 \pm 851.9$  to  $1481.5 \pm 551.7$  cm) and had further worsened at day 56 ( $42.1 \pm 5.5$  s,  $1169.5 \pm 206.3$  cm) (Figure 5a). Importantly,

the locomotor ability of PD mice was significantly improved following the receipt of Venus-mPrestin (N7T, N308S)+US treatment during the experimental period (day 0,  $12.5 \pm 1.4$  s; day 35,  $6.5 \pm 1.4$  s; and day 56,  $7.1 \pm 1.5$  s) (Movie 1). Treating PD mice with US alone was associated with a partial improvement of motor function (day 0,  $7.1 \pm 1.3$  s; day 35,  $13.3 \pm 1.5$  s; and day 56,  $15.5 \pm 2.9$  s). PD mice expressing Venus-mPrestin (N7T, N308S) without US stimulation demonstrated a slight improvement at day 56 ( $12.1 \pm 2.5$  to  $23.3 \pm 5.1$  s). However, expressing Venus alone did not provide any beneficial effect (day 0,  $8.9 \pm 1.7$  s; day 35,  $31.1 \pm 1.4$  s; and day 56,  $42.6 \pm 5.8$  s). Treating PD mice expressing Venus with US produced a partial improvement in locomotor function compared to US alone (day 0,  $7.9 \pm 2.7$  s; day 35,  $8.8 \pm 1.7$  s; and day 56,  $14.4 \pm 2.3$  s).

In the open field test, the Venus-mPrestin (N7T, N308S)+US group similarly showed the most significant improvement in motor activity (day 0,  $5717.2 \pm 471.4$  cm; day

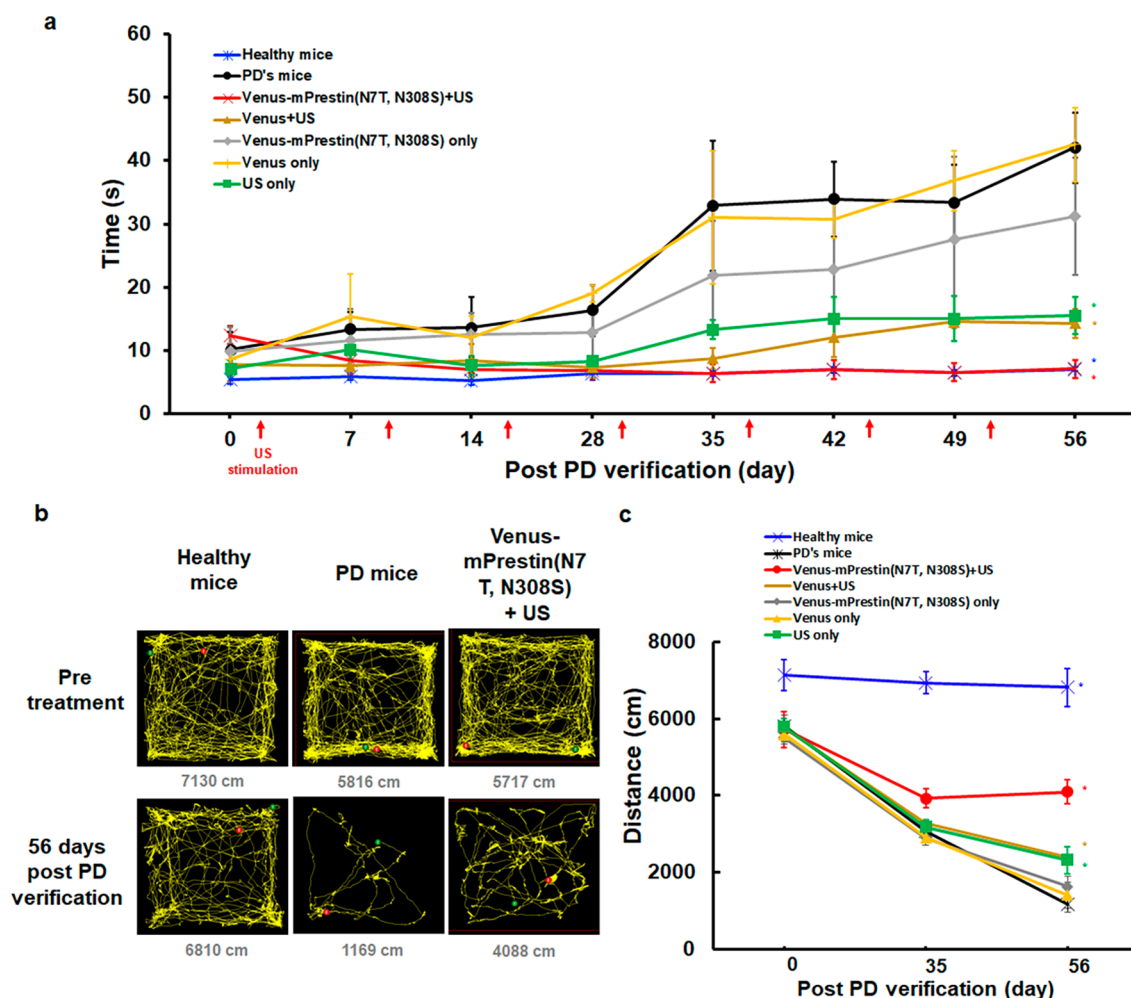


**Figure 5.** Sonogenetic stimulation improved motor function recovery of PD mice. (a) Beam-walking test. Times to cross a beam with a width of 80 cm were recorded to evaluate the motor ability of mice with different treatment protocols. (b) Total trajectory of mice before and after treatment obtained from an open-field test. (c) Total moving distance in 10 min; the distance was normalized to week 0 and defined as the deterioration in evaluating the motor willingness of treated mice (\* $p < 0.05$ )

35,  $3951.6 \pm 199.4$  cm; day 56,  $4088.3 \pm 130.4$  cm; 3.5-fold reduction compared to PD mice without treatment) (Figure 5b,c). The Venus+US group and US-only group showed 2.0-fold ( $5752.8 \pm 325.8$  to  $2390.1 \pm 268.1$  cm) and 1.9-fold ( $5788.1 \pm 209.4$  to  $2417.5 \pm 223.4$  cm) improvements compared to PD mice without treatment at day 56 (Movie 2). The Venus-mPrestin (N7T, N308S)-only group showed a partial improvement in motor function (day 0,  $5497.2 \pm 163.0$  cm; day 35,  $2890.8 \pm 103.0$  cm; and day 56,  $1630.4 \pm 259.1$  cm). The Venus-only group showed severe locomotor function deficits (day 0,  $5587.3 \pm 190.2$  cm; day 35,  $2907.5 \pm 429.9$  cm; and day 56,  $1407.7 \pm 155.6$  cm).

## DISCUSSION

US with microbubbles has been shown to noninvasively target and temporarily open the blood–brain barrier (BBB) for the transport of a neurotrophic (protein or gene) or AAV into the brain, raising the potential of noninvasive neurorestorative effects for PD treatment.<sup>28–30</sup> However, there are four concerns with such methods: (1) Compared with transcranial injection, US-enhanced delivery requires a higher dose of intravenously administered viral vectors or neurotrophic factors (40–1000-fold for neurturin) due to the circulation clearance.<sup>31</sup> The high cost of neurotrophic factors would be

the biggest disadvantage.<sup>30</sup> (2) AAV might still transfect peripheral organs via systemic administration.<sup>31</sup> (3) BBB opening with US might elicit brain inflammation,<sup>32,33</sup> but these inflammatory responses are also beneficial for improving spatial memory in wild-type mice or decreasing the pathological protein load in Alzheimer's disease.<sup>34–37</sup> (4) Providing a tunable system for the spatiotemporal control of neuronal activities with the delivery and expression of therapeutic genes by AAV is challenging. Uncontrollable expression of ectopic neurotrophic factors leads to chronic neuron toxicity.<sup>38</sup> According to our results, one shot of AAV transcranial injection persists in gene expression for at least 8 weeks, which provides a new option for achieving tunable and repeatable neurorestorative effects. This approach offers a promising strategy of long-term clinical neuromodulation with limited invasive procedures.

We observed increased levels of BDNF and NGF after treatment. Possible mechanisms include that the elicited neuron activities would increase the cerebral blood flow because of the extra consumption of oxygen and glucose and then the activation of endothelial cells. The endothelial cells would upregulate endothelial nitric oxide synthase, which is highly correlated with neurotrophin expression and therapy effects.<sup>39,40</sup> In the meantime, the increased cerebral blood flow

would activate astrocytes through the neurovascular coupling response.<sup>41,42</sup> Those astrocytes then secrete several neurotrophins, such as NGF and BDNF.<sup>43,44</sup>

Previous studies have concluded that three mechanisms are probably responsible for the improvement in motor performance in PD mice via US stimulation of the subthalamic nucleus (STN) or globus pallidus (GP): (1) reduced hyperactivity of STN;<sup>45,46</sup> (2) agent delivery to halt retrograde neurodegeneration;<sup>47</sup> and (3) modulation of neural activity in STN or GP causing neuroprotection in PD mice.<sup>48</sup> Therefore, use of the mPrestin ultrasonic system to ameliorate neurodegeneration in the STN or GP is promising.

Previous studies have demonstrated that repeated neuronal stimulation by light promotes recovery following CNS injury, including the following: (1) Stimulating the primary cortex adjacent to the stroke lesion resulted in a significant increase in neuroplasticity markers.<sup>49</sup> (2) Stimulating the phrenic motor neuron following hemisection resulted in a return to normal hemidiaphragm electromyography activity in synchrony with the nonlesioned side.<sup>50</sup> Our results showed that mPrestin could be expressed in dopaminergic neurons as well as in vascular endothelial cells, glutamatergic neurons, and astrocytes.<sup>51</sup> Therefore, it may be possible to apply this new repeated ultrasonic stimulation technique to specific neurons for the treatment of other brain diseases.

We noticed that the expression of Venus-mPrestin (N7T, N308S) without US stimulation also significantly improved the PD symptoms in mice. Although the detailed mechanisms are not clear, it is widely believed that Prestin is important for hearing in outer hair cells by enhancing membrane depolarization.<sup>19,52</sup> This raises the possibility that Prestin in neuron cells may respond to auditory stimulation in the environment.<sup>53,54</sup> The effects of various environmental factors on Prestin-mediated neuromodulation should be comprehensively studied in the future. Moreover, an improvement in dopaminergic neurons was observed in the right SN after US activation on the left SN expressing Venus-mPrestin (N7T, N308S). This is probably achieved by the diffusive neurotrophins triggered by our sonogenetic stimulation. Further studies are needed to clarify this hypothesis.

US wave could have mechanical, cavitation, and thermal effects on biological tissues, potentially inducing an inflammatory response, microhemorrhage, and cellular apoptosis.<sup>55,56</sup> With a set of previously described equations, the currently used US parameters produced an intracerebral temperature increase of only  $5.1 \times 10^{-3}$  °C, which should not induce thermal damage.<sup>57–60</sup> Besides, the acoustic pressure (0.5 MPa) was too low to produce cavitation-related tissue damage (40 MPa, without microbubble injection).<sup>61,62</sup> The mechanical index (MI, 0.7) and  $I_{\text{spta}}$  (68 mW/cm<sup>2</sup>) are far below the upper limit of FDA for clinical ultrasound imaging (MI = 1.9,  $I_{\text{spta}}$  = 720 mW/cm<sup>2</sup>), implying the safety of US stimulation.<sup>63,64</sup> Besides, the histological evaluations revealed that the presence of microglia, macrophages, and apoptotic cells in the left SN of untreated PD mice was probably due to the server degeneration of dopaminergic neurons (Figure S3a). However, in the Venus-mPrestin(N7T, N308S)+US group, the aforementioned cells and erythrocyte extravasation were not observed in the treated area (Figure S3b), confirming the biocompatibility at the tissue level *in vivo*.

## CONCLUSIONS

This study provides a proof of principle for the therapeutic use of sonogenetics to mitigate the neurodegeneration of PD animals. Further work is required to optimize the US parameters for Venus-mPrestin (N7T, N308S) activation and strategies for the gene delivery of brain neurons to further improve therapeutic outcomes. The long-term safety also needs to be considered. These modifications will achieve the goal of the accurate noninvasive modulation of intracerebral neural circuits and may provide a promising therapy for PD patients in the future.

## EXPERIMENTAL SECTION

Please refer to the [Supporting Information](#).

## ASSOCIATED CONTENT

### Supporting Information

The Supporting Information is available free of charge at <https://pubs.acs.org/doi/10.1021/acs.nanolett.1c00886>.

Movie 1: beam-walking tests of an untreated PD mouse and a Venus-mPrestin (N7T, N308S)+US untreated PD mouse (post-PD 56 days) (MOV)

Movie 2: open field tests of an untreated PD mouse, a Venus-mPrestin (N7T, N308S)+US untreated PD mouse, and a healthy mouse (post-PD 56 days) (MOV)

Experimental section, Tables S1 and S2, and Figures S1–S3 (PDF)

## AUTHOR INFORMATION

### Corresponding Authors

Yu-Chun Lin – *Institute of Molecular Medicine and Department of Medical Science, National Tsing Hua University, Hsinchu 30013, Taiwan*; [orcid.org/0000-0002-9629-7560](https://orcid.org/0000-0002-9629-7560); Phone: +886-3-574-2421; Email: [ycl@life.nthu.edu.tw](mailto:ycl@life.nthu.edu.tw)

Chih-Kuang Yeh – *Department of Biomedical Engineering and Environmental Sciences, National Tsing Hua University, Hsinchu 30013, Taiwan*; [orcid.org/0000-0002-2880-6327](https://orcid.org/0000-0002-2880-6327); Phone: +886-3-571-5131; Email: [ckyeh@mx.nthu.edu.tw](mailto:ckyeh@mx.nthu.edu.tw); Fax: +886-3-571-8649

### Authors

Ching-Hsiang Fan – *Department of Biomedical Engineering and Medical Device Innovation Center, National Cheng Kung University, Tainan 70101, Taiwan*

Kuo-Chen Wei – *New Taipei Municipal TuCheng Hospital, New Taipei City 236017, Taiwan*; *Department of Neurosurgery, Chang Gung Memorial Hospital at Linkou, and Chang Gung University, Taoyuan 33305, Taiwan*

Nai-Hua Chiu – *Institute of Nuclear Engineering and Sciences, National Tsing Hua University, Hsinchu 30013, Taiwan*

En-Chi Liao – *Department of Medical Science, Institute of Bioinformatics and Structural Biology, National Tsing Hua University, Hsinchu 30013, Taiwan*

Hsien-Chu Wang – *Institute of Molecular Medicine, National Tsing Hua University, Hsinchu 30013, Taiwan*

Ruo-Yu Wu – *Department of Chemistry, National Taiwan University, Taipei 106319, Taiwan*

Yi-Ju Ho – *Department of Biomedical Engineering and Environmental Sciences, National Tsing Hua University, Hsinchu 30013, Taiwan*

**Hong-Lin Chan** – Department of Medical Science, Institute of Bioinformatics and Structural Biology, National Tsing Hua University, Hsinchu 30013, Taiwan

**Tsung-Shing Andrew Wang** – Department of Chemistry, National Taiwan University, Taipei 106319, Taiwan

**Ying-Zu Huang** – Neuroscience Research Center, Healthy Aging Research Center and Department of Neurology, Chang Gung Memorial Hospital and Chang Gung University College of Medicine, Taoyuan 33305, Taiwan

**Tsung-Hsun Hsieh** – School of Physical Therapy, Healthy Aging Research Center & Neuroscience Research Center, Chang Gung Memorial Hospital and Chang Gung University College of Medicine, Taoyuan 33305, Taiwan

**Chin-Hsien Lin** – Department of Neurology, National Taiwan University Hospital, College of Medicine, National Taiwan University, Taipei 106319, Taiwan

Complete contact information is available at:

<https://pubs.acs.org/10.1021/acs.nanolett.1c00886>

### Author Contributions

▲C.-H. Fan and K.-C. Wei contributed equally to this work.

### Author Contributions

C.-H.F., K.-C.W., Y.-J.H., Y.-C.L., and C.-K.Y. designed the experiments. C.-H.F. and N.-H.C. programmed the ultrasound system under the supervision of K.-C.W., Y.-C.L., and C.-K.Y., H.-C.W., R.-Y.W., T.-S.A.W., and Y.-C.L. performed the cell biology experiments. C.-H.F., N.-H.C., H.-C.W., and E.-C.L. quantified the imaging results. N.-H.C. and Y.-C.L. generated the DNA constructs. N.-H.C. and E.-C.L. performed the Western blot analysis. N.-H.C. performed the animal behavior tests under the supervision of Y.-Z.H., and T.-H.H. performed the animal experiments. C.-H.F., K.-C.W., Y.-J.H., C.-H.L., Y.-C.L., and C.-K.Y. wrote the paper.

### Funding

This study is sponsored by the Ministry of Science and Technology, Taiwan (grants 108-2221-E-007-041-MY3, 108-2221-E-007-040-MY3, 108-2638-M-002-001-MY2, 108-2638-B-010-001-MY2, 109-2636-E-006-024, 110-2636-B-007-011-, and 110-2321-B-002-010), National Tsing Hua University (Hsinchu, Taiwan) under grant no. 109Q2511E1, Chang Gung Memorial Hospital (Taoyuan, Taiwan) under grant no. CORPG3K0091, and the Higher Education Sprout Project, Ministry of Education to the Headquarters of University Advancement from National Cheng Kung University.

### Notes

The authors declare no competing financial interest.

### ACKNOWLEDGMENTS

The authors gratefully acknowledge the support of Professors C.-W. Chang and Y.-F. Huang for their help with the experiments.

### ABBREVIATIONS

CNS, central nerve system; PD, Parkinson's disease; SN, substantia nigra; US, ultrasound; BDNF, brain-derived neurotrophic factor; AAV, adeno-associated virus; TH, tyrosine hydroxylase; NGF, nerve growth factor; BBB, blood–brain barrier; STN, subthalamic nucleus; GP, globus pallidus; MI, mechanical index

### REFERENCES

- (1) Dauer, W.; Przedborski, S. Parkinson's disease: mechanisms and models. *Neuron* **2003**, *39* (6), 889–909.
- (2) Lang, A. E.; Lozano, A. M. Parkinson's disease. *N. Engl. J. Med.* **1998**, *339* (16), 1130–1143.
- (3) LeWitt, P. A. Levodopa therapy for Parkinson's disease: pharmacokinetics and pharmacodynamics. *Mov. Disord.* **2015**, *30* (1), 64–72.
- (4) Weaver, F. M.; Follett, K. A.; Stern, M.; Luo, P.; Harris, C. L.; Hur, K.; Marks, W. J.; Rothlind, J.; Sagher, O.; Moy, C. Randomized trial of deep brain stimulation for Parkinson disease: thirty-six-month outcomes. *Neurology* **2012**, *79* (1), 55–65.
- (5) Zhuang, X.; Mazzoni, P.; Kang, U. J. The role of neuroplasticity in dopaminergic therapy for Parkinson disease. *Nat. Rev. Neurol.* **2013**, *9* (5), 248–56.
- (6) Qi, C.; Varga, S.; Oh, S. J.; Lee, C. J.; Lee, D. Optogenetic Rescue of Locomotor Dysfunction and Dopaminergic Degeneration Caused by Alpha-Synuclein and EKO Genes. *Exp Neurol* **2017**, *26* (2), 97–103.
- (7) Howe, M. W.; Dombeck, D. A. Rapid signalling in distinct dopaminergic axons during locomotion and reward. *Nature* **2016**, *535* (7613), 505–10.
- (8) Yang, F. Y.; Lu, W. W.; Lin, W. T.; Chang, C. W.; Huang, S. L. Enhancement of Neurotrophic Factors in Astrocyte for Neuroprotective Effects in Brain Disorders Using Low-intensity Pulsed Ultrasound Stimulation. *Brain Stimul* **2015**, *8* (3), 465–73.
- (9) Tufail, Y.; Matyushov, A.; Baldwin, N.; Tauchmann, M. L.; Georges, J.; Yoshihiro, A.; Tillery, S. I.; Tyler, W. J. Transcranial pulsed ultrasound stimulates intact brain circuits. *Neuron* **2010**, *66* (5), 681–94.
- (10) Fox, M. W.; Ahlskog, J. E.; Kelly, P. J. Stereotactic ventrolateral thalamotomy for medically refractory tremor in post-levodopa era Parkinson's disease patients. *J. Neurosurg.* **1991**, *75* (5), 723–30.
- (11) Jankovic, J.; Cardoso, F.; Grossman, R. G.; Hamilton, W. J. Outcome after stereotactic thalamotomy for parkinsonian, essential, and other types of tremor. *Neurosurgery* **1995**, *37* (4), 680–6. discussion 686–7.
- (12) Ordaz, J. D.; Wu, W.; Xu, X.-M. Optogenetics and its application in neural degeneration and regeneration. *Neural Regen. Res.* **2017**, *12* (8), 1197.
- (13) Steinbeck, J. A.; Choi, S. J.; Mrejeru, A.; Ganat, Y.; Deisseroth, K.; Sulzer, D.; Mosharov, E. V.; Studer, L. Optogenetics enables functional analysis of human embryonic stem cell–derived grafts in a Parkinson's disease model. *Nat. Biotechnol.* **2015**, *33* (2), 204.
- (14) Crisci, A. R.; Ferreira, A. L. Low-intensity pulsed ultrasound accelerates the regeneration of the sciatic nerve after neurotomy in rats. *Ultrasound in medicine & biology* **2002**, *28* (10), 1335–1341.
- (15) Scarcelli, T.; Jordão, J. F.; O'reilly, M. A.; Ellens, N.; Hynynen, K.; Aubert, I. Stimulation of hippocampal neurogenesis by transcranial focused ultrasound and microbubbles in adult mice. *Brain stimulation* **2014**, *7* (2), 304–307.
- (16) Su, W.-S.; Wu, C.-H.; Chen, S.-F.; Yang, F.-Y. Low-intensity pulsed ultrasound improves behavioral and histological outcomes after experimental traumatic brain injury. *Sci. Rep.* **2017**, *7* (1), 15524.
- (17) Huang, S.-L.; Chang, C.-W.; Lee, Y.-H.; Yang, F.-Y. Protective effect of low-intensity pulsed ultrasound on memory impairment and brain damage in a rat model of vascular dementia. *Radiology* **2017**, *282* (1), 113–122.
- (18) Huang, Y. S.; Fan, C. H.; Hsu, N.; Chiu, N. H.; Wu, C. Y.; Chang, C. Y.; Wu, B. H.; Hong, S. R.; Chang, Y. C.; Yan-Tang Wu, A.; Guo, V.; Chiang, Y. C.; Hsu, W. C.; Chen, L.; Pin-Kuang Lai, C.; Yeh, C. K.; Lin, Y. C. Sonogenetic Modulation of Cellular Activities Using an Engineered Auditory-Sensing Protein. *Nano Lett.* **2020**, *20* (2), 1089–1100.
- (19) Ludwig, J.; Oliver, D.; Frank, G.; Klöcker, N.; Gummer, A. W.; Fakler, B. Reciprocal electromechanical properties of rat prestin: the motor molecule from rat outer hair cells. *Proc. Natl. Acad. Sci. U. S. A.* **2001**, *98* (7), 4178–83.



- (20) Fettiplace, R.; Hackney, C. M. The sensory and motor roles of auditory hair cells. *Nat. Rev. Neurosci.* **2006**, *7* (1), 19–29.
- (21) Li, Y. Y.; Liu, Z.; Qi, F. Y.; Zhou, X.; Shi, P. Functional Effects of a Retained Ancestral Polymorphism in Prestin. *Mol. Biol. Evol.* **2017**, *34* (1), 88–92.
- (22) Abdelfattah, A. S.; Kawashima, T.; Singh, A.; Novak, O.; Liu, H.; Shuai, Y.; Huang, Y. C.; Campagnola, L.; Seeman, S. C.; Yu, J.; Zheng, J.; Grimm, J. B.; Patel, R.; Friedrich, J.; Mensh, B. D.; Paninski, L.; Macklin, J. J.; Murphy, G. J.; Podgorski, K.; Lin, B. J.; Chen, T. W.; Turner, G. C.; Liu, Z.; Koyama, M.; Svoboda, K.; Ahrens, M. B.; Lavis, L. D.; Schreier, E. R. Bright and photostable chemigenetic indicators for extended in vivo voltage imaging. *Science* **2019**, *365* (6454), 699–704.
- (23) Gjedde, A.; Léger, G. C.; Cumming, P.; Yasuhara, Y.; Evans, A. C.; Guttman, M.; Kuwabara, H. Striatal L-dopa decarboxylase activity in Parkinson's disease in vivo: implications for the regulation of dopamine synthesis. *J. Neurochem.* **1993**, *61* (4), 1538–41.
- (24) Melamed, E.; Hefti, F.; Wurtman, R. J. Nonaminergic striatal neurons convert exogenous L-dopa to dopamine in parkinsonism. *Ann. Neurol.* **1980**, *8* (6), 558–63.
- (25) Ekstrand, M. I.; Galter, D. The MitoPark Mouse - an animal model of Parkinson's disease with impaired respiratory chain function in dopamine neurons. *Parkinsonism Relat Disord* **2009**, *15* (Suppl 3), S185.
- (26) Galter, D.; Pernold, K.; Yoshitake, T.; Lindqvist, E.; Hoffer, B.; Kehr, J.; Larsson, N. G.; Olson, L. MitoPark mice mirror the slow progression of key symptoms and L-DOPA response in Parkinson's disease. *Genes, Brain Behav.* **2010**, *9* (2), 173–81.
- (27) Ekstrand, M. I.; Terzioglu, M.; Galter, D.; Zhu, S.; Hofstetter, C.; Lindqvist, E.; Thams, S.; Bergstrand, A.; Hansson, F. S.; Trifunovic, A.; Hoffer, B.; Cullheim, S.; Mohammed, A. H.; Olson, L.; Larsson, N. G. Progressive parkinsonism in mice with respiratory-chain-deficient dopamine neurons. *Proc. Natl. Acad. Sci. U. S. A.* **2007**, *104* (4), 1325–30.
- (28) Lin, C. Y.; Lin, Y. C.; Huang, C. Y.; Wu, S. R.; Chen, C. M.; Liu, H. L. Ultrasound-responsive neurotrophic factor-loaded microbubble-liposome complex: Preclinical investigation for Parkinson's disease treatment. *J. Controlled Release* **2020**, *321*, 519–528.
- (29) Yue, P.; Gao, L.; Wang, X.; Ding, X.; Teng, J. Ultrasound-triggered effects of the microbubbles coupled to GDNF- and Nurr1-loaded PEGylated liposomes in a rat model of Parkinson's disease. *J. Cell. Biochem.* **2018**, *119* (6), 4581–4591.
- (30) Karakatsani, M. E.; Wang, S.; Samiotaki, G.; Kugelmann, T.; Olumolade, O. O.; Acosta, C.; Sun, T.; Han, Y.; Kamimura, H. A. S.; Jackson-Lewis, V.; Przedborski, S.; Konofagos, E. Amelioration of the nigrostriatal pathway facilitated by ultrasound-mediated neurotrophic delivery in early Parkinson's disease. *J. Controlled Release* **2019**, *303*, 289–301.
- (31) Thévenot, E.; Jordão, J. F.; O'Reilly, M. A.; Markham, K.; Weng, Y. Q.; Foust, K. D.; Kaspar, B. K.; Hynynen, K.; Aubert, I. Targeted delivery of self-complementary adeno-associated virus serotype 9 to the brain, using magnetic resonance imaging-guided focused ultrasound. *Hum. Gene Ther.* **2012**, *23* (11), 1144–55.
- (32) Kovacs, Z. I.; Kim, S.; Jikaria, N.; Qureshi, F.; Milo, B.; Lewis, B. K.; Bresler, M.; Burks, S. R.; Frank, J. A. Disrupting the blood-brain barrier by focused ultrasound induces sterile inflammation. *Proc. Natl. Acad. Sci. U. S. A.* **2017**, *114* (1), E75–e84.
- (33) Kovacs, Z. I.; Tu, T. W.; Sundby, M.; Qureshi, F.; Lewis, B. K.; Jikaria, N.; Burks, S. R.; Frank, J. A. MRI and histological evaluation of pulsed focused ultrasound and microbubbles treatment effects in the brain. *Theranostics* **2018**, *8* (17), 4837–4855.
- (34) Shen, Y.; Hua, L.; Yeh, C. K.; Shen, L.; Ying, M.; Zhang, Z.; Liu, G.; Li, S.; Chen, S.; Chen, X.; Yang, X. Ultrasound with microbubbles improves memory, ameliorates pathology and modulates hippocampal proteomic changes in a triple transgenic mouse model of Alzheimer's disease. *Theranostics* **2020**, *10* (25), 11794–11819.
- (35) Shin, J.; Kong, C.; Lee, J.; Choi, B. Y.; Sim, J.; Koh, C. S.; Park, M.; Na, Y. C.; Suh, S. W.; Chang, W. S.; Chang, J. W. Focused ultrasound-induced blood-brain barrier opening improves adult hippocampal neurogenesis and cognitive function in a cholinergic degeneration dementia rat model. *Alzheimer's Res. Ther.* **2019**, *11* (1), 110.
- (36) Burgess, A.; Dubey, S.; Yeung, S.; Hough, O.; Eterman, N.; Aubert, I.; Hynynen, K. Alzheimer disease in a mouse model: MR imaging-guided focused ultrasound targeted to the hippocampus opens the blood-brain barrier and improves pathologic abnormalities and behavior. *Radiology* **2014**, *273* (3), 736–45.
- (37) Leinenga, G.; Götz, J. Scanning ultrasound removes amyloid- $\beta$  and restores memory in an Alzheimer's disease mouse model. *Sci. Transl. Med.* **2015**, *7* (278), 278ra33.
- (38) Luz, M.; Mohr, E.; Fibiger, H. C. GDNF-induced cerebellar toxicity: A brief review. *NeuroToxicology* **2016**, *52*, 46–56.
- (39) Eguchi, K.; Shindo, T.; Ito, K.; Ogata, T.; Kurosawa, R.; Kagaya, Y.; Monma, Y.; Ichijo, S.; Kasukabe, S.; Miyata, S.; Yoshikawa, T.; Yanai, K.; Taki, H.; Kanai, H.; Osumi, N.; Shimokawa, H. Whole-brain low-intensity pulsed ultrasound therapy markedly improves cognitive dysfunctions in mouse models of dementia - Crucial roles of endothelial nitric oxide synthase. *Brain Stimul* **2018**, *11* (5), 959–973.
- (40) Albrecht, E. W.; Stegeman, C. A.; Heeringa, P.; Henning, R. H.; van Goor, H. Protective role of endothelial nitric oxide synthase. *J. Pathol.* **2003**, *199* (1), 8–17.
- (41) Brocka, M.; Helbing, C.; Vincenz, D.; Scherf, T.; Montag, D.; Goldschmidt, J.; Angenstein, F.; Lippert, M. Contributions of dopaminergic and non-dopaminergic neurons to VTA-stimulation induced neurovascular responses in brain reward circuits. *NeuroImage* **2018**, *177*, 88–97.
- (42) Iordanova, B.; Vazquez, A.; Kozai, T. D.; Fukuda, M.; Kim, S. G. Optogenetic investigation of the variable neurovascular coupling along the interhemispheric circuits. *J. Cereb. Blood Flow Metab.* **2018**, *38* (4), 627–640.
- (43) Liu, S. H.; Lai, Y. L.; Chen, B. L.; Yang, F. Y. Ultrasound Enhances the Expression of Brain-Derived Neurotrophic Factor in Astrocyte Through Activation of TrkB-Akt and Calcium-CaMK Signaling Pathways. *Cereb Cortex* **2016**, *27* (6), 3152–3160.
- (44) Zhao, L.; Feng, Y.; Hu, H.; Shi, A.; Zhang, L.; Wan, M. Low-Intensity Pulsed Ultrasound Enhances Nerve Growth Factor-Induced Neurite Outgrowth through Mechanotransduction-Mediated ERK1/2-CREB-Trx-1 Signaling. *Ultrasound Med. Biol.* **2016**, *42* (12), 2914–2925.
- (45) Elias, W. J.; Lipsman, N.; Ondo, W. G.; Ghanouni, P.; Kim, Y. G.; Lee, W.; Schwartz, M.; Hynynen, K.; Lozano, A. M.; Shah, B. B.; Huss, D.; Dallapiazza, R. F.; Gwinn, R.; Witt, J.; Ro, S.; Eisenberg, H. M.; Fishman, P. S.; Gandhi, D.; Halpern, C. H.; Chuang, R.; Butts Pauly, K.; Tierney, T. S.; Hayes, M. T.; Cosgrove, G. R.; Yamaguchi, T.; Abe, K.; Taira, T.; Chang, J. W. A Randomized Trial of Focused Ultrasound Thalamotomy for Essential Tremor. *N. Engl. J. Med.* **2016**, *375* (8), 730–9.
- (46) Lipsman, N.; Schwartz, M. L.; Huang, Y.; Lee, L.; Sankar, T.; Chapman, M.; Hynynen, K.; Lozano, A. M. MR-guided focused ultrasound thalamotomy for essential tremor: a proof-of-concept study. *Lancet Neurol.* **2013**, *12* (5), 462–8.
- (47) Wang, X.; Cui, G.; Yang, X.; Zhang, Z.; Shi, H.; Zu, J.; Hua, F.; Shen, X. Intracerebral administration of ultrasound-induced dissolution of lipid-coated GDNF microbubbles provides neuroprotection in a rat model of Parkinson's disease. *Brain Res. Bull.* **2014**, *103*, 60–5.
- (48) Zhou, H.; Niu, L.; Meng, L.; Lin, Z.; Zou, J.; Xia, X.; Huang, X.; Zhou, W.; Bian, T.; Zheng, H. Noninvasive Ultrasound Deep Brain Stimulation for the Treatment of Parkinson's Disease Model Mouse. *Research (Wash D C)* **2019**, *2019*, 1748489.
- (49) Cheng, M. Y.; Wang, E. H.; Woodson, W. J.; Wang, S.; Sun, G.; Lee, A. G.; Arac, A.; Fenno, L. E.; Deisseroth, K.; Steinberg, G. K. Optogenetic neuronal stimulation promotes functional recovery after stroke. *Proc. Natl. Acad. Sci. U. S. A.* **2014**, *111* (35), 12913–8.

- (50) Alilain, W. J.; Li, X.; Horn, K. P.; Dhingra, R.; Dick, T. E.; Herlitze, S.; Silver, J. Light-induced rescue of breathing after spinal cord injury. *J. Neurosci.* **2008**, *28* (46), 11862–70.
- (51) Wu, C. Y.; Fan, C. H.; Chiu, N. H.; Ho, Y. J.; Lin, Y. C.; Yeh, C. K. Targeted delivery of engineered auditory sensing protein for ultrasound neuromodulation in the brain. *Theranostics* **2020**, *10* (8), 3546–3561.
- (52) Liu, Z.; Qi, F. Y.; Zhou, X.; Ren, H. Q.; Shi, P. Parallel sites implicate functional convergence of the hearing gene prestin among echolocating mammals. *Mol. Biol. Evol.* **2014**, *31* (9), 2415–24.
- (53) Dallos, P.; Fakler, B. Prestin, a new type of motor protein. *Nat. Rev. Mol. Cell Biol.* **2002**, *3* (2), 104–11.
- (54) Dallos, P. Cochlear amplification, outer hair cells and prestin. *Curr. Opin. Neurobiol.* **2008**, *18* (4), 370–6.
- (55) ter Haar, G. Ultrasound bioeffects and safety. *Proc. Inst. Mech. Eng., Part H* **2010**, *224* (2), 363–373.
- (56) Elias, W. J.; Huss, D.; Voss, T.; Loomba, J.; Khaled, M.; Zadicario, E.; Frysinger, R. C.; Sperling, S. A.; Wylie, S.; Monteith, S. J.; Druzgal, J.; Shah, B. B.; Harrison, M.; Wintermark, M. A pilot study of focused ultrasound thalamotomy for essential tremor. *N. Engl. J. Med.* **2013**, *369* (7), 640–8.
- (57) O'Brien, W. D., Jr. Ultrasound-biophysics mechanisms. *Prog. Biophys. Mol. Biol.* **2007**, *93* (1–3), 212–55.
- (58) Cooper, T. E.; Trezek, G. J. A probe technique for determining the thermal conductivity of tissue. *J. Heat Transfer* **1972**, *94*, 133–140.
- (59) Nyborg, W. L. Heat generation by ultrasound in a relaxing medium. *J. Acoust. Soc. Am.* **1981**, *70* (2), 310–312.
- (60) Goss, S. A.; Johnston, R. L.; Dunn, F. Comprehensive compilation of empirical ultrasonic properties of mammalian tissues. *J. Acoust. Soc. Am.* **1978**, *64* (2), 423–57.
- (61) Dalecki, D. Mechanical bioeffects of ultrasound. *Annu. Rev. Biomed. Eng.* **2004**, *6*, 229–48.
- (62) Tyler, W. J.; Tufail, Y.; Finsterwald, M.; Tauchmann, M. L.; Olson, E. J.; Majestic, C. Remote excitation of neuronal circuits using low-intensity, low-frequency ultrasound. *PLoS One* **2008**, *3* (10), e3511.
- (63) Duck, F. A. Acoustic saturation and output regulation. *Ultrasound Med. Biol.* **1999**, *25* (6), 1009–18.
- (64) Deffieux, T.; Younan, Y.; Wattiez, N.; Tanter, M.; Pouget, P.; Aubry, J. F. Low-intensity focused ultrasound modulates monkey visuomotor behavior. *Curr. Biol.* **2013**, *23* (23), 2430–3.